Available online at www.sciencedirect.com

ScienceDirect

Procedia Structural Integrity 34 (2021) 266–273

Structural Integrity Procedia

www.elsevier.com/locate/procedia

The second European Conference on the Structural Integrity of Additively Manufactured Materials

Finish-pass strategy to improve sidewall angle and processing time in FIB milled structures

Markus Joakim Lid[a,*], Abdulla Bin Afif[a], Jan Torgersen[a], Fritz B. Prinz[b]

[a]*Department of Mechanical and Industrial Engineering, Norwegian University of Science and Technology, NTNU, 7491 Trondheim, Norway*
[b]*Department of Mechanical Engineering, Stanford University, Stanford, California 94305, USA*

Abstract

Focused Ion Beams (FIB) systems are employed for their ability to manipulate and remove material on the nanoscale for creating complex structures. By splitting the milling job into multiple sub-patterns, consisting of a bulk milling pattern, and one or more finish pass patterns that follow the contours of the milling geometry, we show that one can counteract the effect of re-deposition on the sidewalls. Our tests showed a reduction in sidewall angle from 96°to 92.5°using identical beam conditions and nearly the same processing time employing only one finish pass pattern. Further, by assigning different beam currents to three different sub-patterns, we were able to reduce angles to 92°, while cutting total milling time by 10%. Improving our strategy may render FIB systems a potential as effective nanofabrication tools applicable beyond creating prototypes and lamellae for material characterization.

Keywords: Focused Ion Beam milling; pattern generation; processing time

1. Introduction

Focused Ion Beam (FIB) has a wide range of uses within several fields of science and engineering. The finely focused ion beam is used to alter the target material, mainly through localized sputtering referred to as FIB milling. Within material science, it is perhaps most established for making thin lamellae from material substrates for characterization with transition electron microscopes (TEM). It is also used for creating samples for atom probe microscopy and allows slice and view operations for tomographic characterization. It also widely used within the semiconductor industry for failure analysis, as it can easily mill through structures and make pattern metal and insulating contacts on the fly. It is nearly the only available technique for creating micro-pillars and cantilever beams for nano-mechanical testing. The FIB is also a great tool for creating structures from a predefined design, where it is conveniently used for prototyping structures in micro-electronic mechanical systems (MEMS), and photonic circuits.

* Corresponding author.
E-mail address: markus.j.lid@ntnu.no

2452-3216
10.1016/j.prostr.2021.12.038

The most obvious artifact from FIB milling is that of redeposition of sputtered material. As the energetic ion is colliding with target atoms, enough energy can be transferred to the atom to surpass the surface binding energy, causing surface atoms to be sputtered. If a solid surface is in the trajectory of the sputtered atoms, a fraction of the sputtered atoms may bind to the surface, which is known as redeposition. The direction of which sputtering is occurring, the sputter angle distribution, is mostly dependent on the angle of incidence between the ion beam and the target surface normal. Since the surface contour is continually altered during the milling, the chosen milling patterns and milling strategy will alter how much, and where redeposition occurs. A milling pattern that is based on offsets of the surface contour will have a smaller amount of redeposition on the sidewalls compared to a pattern that simply consists of parallel lines Yoon et al. (2017).

Besides setting the scanning path to have material sputter confined to a desired direction, one or more separate patterns may be applied afterwards that are known as cleaning cross-section (CCS). A CCS consists of a set of parallel lines that are scanned one by one with a longer dwell time. This will give straighter wall segments with minimal amount of redeposited material on the finished wall. Also, these patterns will typically be applied with a lower acceleration voltage (AV), as a lower energy beam will cause a thinner damage layer on the finished surface. This is the typical approach for creating TEM samples, where the goal is to characterize the material with minimal amounts of beam damage from FIB milling. The same is true for atom probe tomography, where instead of parallel lines, circular scan lines are used with a radial offset to create a circular pillar. While the cleaning walls are easily applied to simple geometries such as lamellae and circular pillars, it is more difficult to apply to complex shapes. Bachmann (2020) created a sample with multiple trenches to measure conductivity, where a pattern was first constructed by regular milling, and subsequently applied a set of multiple CCSs along every straight wall segment. In principle, this provides a viable solution as long as the desired patterns are straight wall segments. However, it becomes difficult to make for a complicated design consisting of multiple wall segments, and if the patterns are not milled in parallel, there could be a significant amount of redeposited material on a section adjecent to the currently milling CCS.

While the most common patterns that can be created with the most common FIB software consist of rectangles, and circles, and combined shapes from these primitives, patterning software such as NanoBuilder allows the user to import GDSII files containing 2D geometries defined in other CAD software. However, the rasterization options for such shapes will be limited to parallel scan lines within the geometry boundary, and are thus neither capable of benefiting from a scan path which is based on offsets from the boundary contour, or benefiting from finish passes. Another patterning option is using bitmap files, where the image intensities correspond to a varying dwell time. This approach has, for instance, seen use cases for creating curved surfaces Chen et al. (2020). While giving a greater design space to customize the milling, it still relies on a raster scanning pattern. The biggest freedom comes from directly controlling the beam path, through defining coordinates and dwell times of individual dwell sites. These patterns will have to be created externally by third party software and imported to the FIB software in specific files.

There have been several approaches to creating stream files. Some available codes create arrays of nanoholes or V-groove trenches Cui et al. (2017). Niessen and Nancarrow (2019) used traditional CAD software for designing geometry and created G-code files for a milling operation where the tool radius is comparable to beam size though a scaling factor, and then through a MATLAB script, translate the G-code to a stream file. While this is an interesting approach, especially for someone already familiar with CAD/CAM software, the workflow has several quirks and impracticalities. Recently, Deinhart et al. (2021) has created a new software called FIB-o-mat for creating custom stream files. It is available as a Python package and allows a low-level patterning approach where the user has a vast amount of options to custom define the beam path for a given geometry, and to create automated patterning through Python scripts.

In this paper, we present a patterning strategy where the milling job is split into boundary-offsetted patterns and finish passes. We create the patterns using the FIB-o-mat toolbox. We show the viability of our algorithm, and demonstrate how it performs when applied to a test geometry with multiple corners curved edges. We use sidewall angle as a qualitative measure to milling quality. The beam current has a strong correlation with the milling rate, and thus with total processing time. Since the quality of many patterns may be improved by reducing the beam current due to a smaller beam diameter and reduced artifacts from sample heating, we evaluate the finished quality in light of milling time, as the milling time is directly linked to the cost of processing.

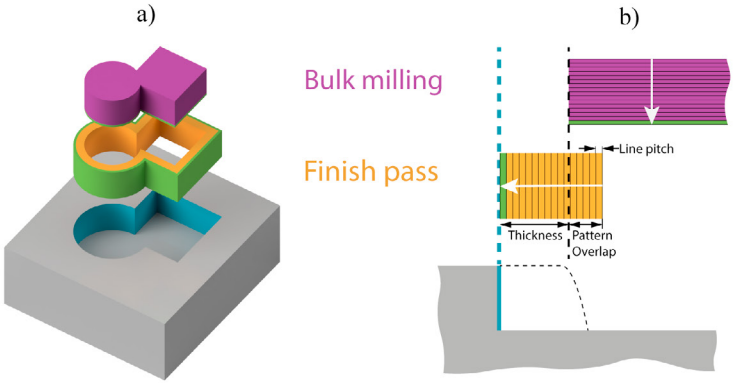

Fig. 1. Milling strategy for enhanced dimensional accuracy of side wall by separating the milling into bulk milling, and wall finishing steps. (a) Explosion view of the milling volumes in the target material. Topmost shape (purple) shows the bulk milling volume which is offset inwards compared to the target boundary. Below the milling volume corresponding to the sidewall finish passes is illustrated. (b) Diagram showing milling profile with respect to target geometry sidewall (turquoise line). Topmost block (purple) corresponds to the bulk milling, and is milled layer by layer parallel to top surface, whereas the wall finish (orange) is milled in layers offset to boundary walls

2. Methods

2.1. Milling target

Consecutive layers of Pt, Al, Pt, Al, Pt were deposited on a silicon wafer with crystal structure aligned in the [001] direction, using electron-beam evaporation (AJA International Inc) at a deposition rate of 5 Å/s, each layer at 20 nm thickness. The reason for using these layers on top is that platinum and aluminum sputters at a rate close to that of silicon, but differs greatly in secondary electron yield which can be seen in table 1, which should give them a strong contrast during SEM imaging. Some typical values for sputter rate, given as volume removed material per ion dose at 30 kV, and secondary electron yield is given in table 1. These layers on top help give an accurate reference to the top surface, and give better visual queues to the geometry of the top edge along a pattern boundary.

Table 1. Values for sputter rate secondary electron yield

Material	Sputter rate (μm^3/nC)	Ref.	δ at 2 keV	Ref.
Silicon	0.24	Mulders et al. (2007)	0.44	Lin and Joy (2005)
Aluminum	0.29	Mulders et al. (2007)	0.84	Lin and Joy (2005)
Platinum	0.23	Utke et al. (2012)	1.22	Lin and Joy (2005)

2.2. Milling pattern

The patterns are created with custom functions based on FIB-o-mat functions called *curve_tools.deflate()*, which create scan lines with a given offset boundary separated by a line pitch, P_{line}, until whole geometry is filled with offsets. The scan is set to start at the innermost offset, and progress towards the boundary. The scan line is rasterized to individual points along the line in consecutive order, with raster pitch P_{raster}. These patterns can either fill a hole geometry and be repeated a set number of times with a short dwell time to make a bulk mill pattern, or to span over a smaller offset distance and a single repeat to create a finish pass. The functions take the pitch as input, but when patterning with FIB it is common practice to define scanning parameters in terms of scanning overlap as a function of the beam size. The pitch is defined as

$$P_i = D_{beam}\,(1 - f_i) \tag{1}$$

where D_{beam} is the beam diameter given by the full-width at half-maximum (FWHM) of the beam distribution. There are established methods to measure the beam distribution, and calculate the FWHM value, with knife edge method [reference], but for this work the beam diameter is simply used as specified in the FIB software. The reason for defining the pitch in terms of beam overlap, is that it helps to create patterns with a similar milling behaviour across multiple beam conditions.

The different steps, which are separated into bulk milling and wall finishing steps are created by the same overall patterning technique, but differ when it comes to the dwell-time at the individual dwell sites. Bulk milling uses short dwell-time, and repeats the pattern over and over again, while wall finish pass uses a long dwell time and a higher overlap ratio, repeating the pattern only once. The flux is given by

$$F = \frac{I_{ion} t_{tot}}{A} \tag{2a}$$

$$= \frac{I_{ion} t_{spot} n_{reps}}{P_{line} P_{rast}} \tag{2b}$$

where n_reps is the number of pattern repetitions. Going from 2a to 2b assumes, a small curvature of scan line compared to P_rast. Now the number of pattern repetitions can be calculated for bulk milling step by solving 2b with respect to n_{reps}

$$n_{reps} = \frac{F P_{line} P_{rast}}{I_{ion} t_{spot}} \tag{3}$$

and the dwell-time for wall finish pass is given by:

$$t_{spot} = \frac{F P_{line} P_{rast}}{I_{ion} n_{linereps}} \tag{4}$$

Where n_{reps} is replaced by $n_{linereps}$, which is the number of times the beam is scanning a single line, before progressing to the next line.

Three different milling sites were made with the same boundary geometry, naming them $A1$, $A2$ and $A3$. $A1$ is made purely with bulk milling, $A2$ is split into two sub patterns, with bulk milling and subsequent finish pass using the same beam current as $A1$, while $A3$ is split wall finish into two separate patterns with all three patterns having different beam current. The pattern is created as defined in 2. All patterns are milled using 30 kV, and rastering overlap of 50%, with a flux of 5 nC/μm^2. For the parameters that are varying are specified in 2. We made a custom script to convert the patterning file to the patterning format compatible with FEI instruments, called Stream file.

2.3. FIB milling

FEI Helios G4 DualBeam SEM/FIB with a conventional gallium beam is used. FEI NanoBuilder software is used to execute patterning with the FIB. NanoBuilder allows extended functionality beyond that of the regular Microscope Control software, especially when several patterns are used in the same job. Multiple patterns can be applied to different layers, that are executed at different beam conditions with alignment capabilities, which might be necessary when multiple beam conditions are used in the same job, or if the sample is prone to drifting. Sample $A1$ and $A2$ use only one beam condition for the same job, so no alignment is needed. $A3$ uses three different beam conditions, so an alignment is necessary between executing each sub-job. We have done this by patterning a square and circle within the same field of view as the pattern is placed, and telling NanoBuilder to align according to this feature. Between each executed layer, NanoBuilder will change the beam and wait for it to stabilize. Then it scans over a predefined scan

Table 2. FIB patterning settings. Values enclosed by parenthesis are implicitly defined based on the other values in the table, which are set explicitly.

Mill job	BC	D_{beam}	f_{line}	W_{width}	$W_{overlap}$	t_{dwell}	n_{reps}	n_{line}
A1-B	260 pA	(36.6 nm)	50%	~	~	1 us	(6440)	1
A2-B	260 pA	(36.6 nm)	50%	~	~	1 us	(6440)	1
A2-FP1	260 pA	(36.6 nm)	75%	80 nm	50 nm	(644 us)	1	5
A3-B	750 pA	(66.2 nm)	50%	~	~	1 us	(7304)	5
A3-FP1	260 pA	(36.6 nm)	75%	30 nm	100 nm	(644 us)	1	5
A3-FP2	41 pA	(15.0 nm)	75%	30 nm	20 nm	(686 us)	1	5

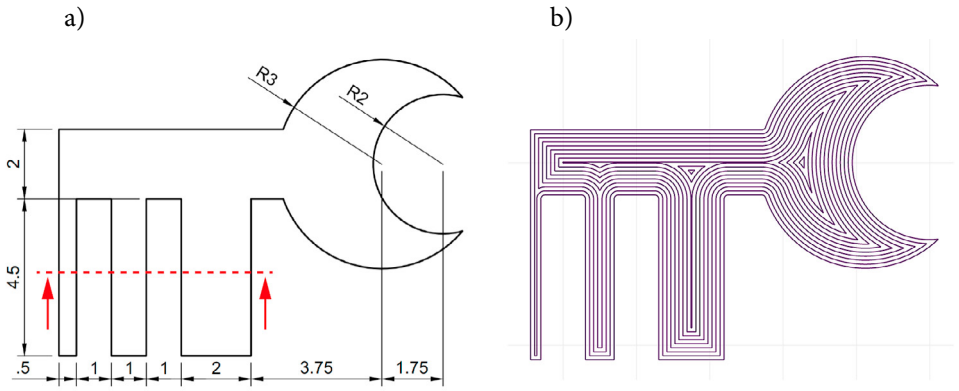

Fig. 2. a) Drawing of the 2D geometry showing the dimensions used. All dimensions are given in micrometers. The red line indicates where the cross sections are made, and red arrows show in which direction they are viewed. b) Showing similar scanlines as used in sample $A1$, except the pitch is multiplied by a factor of 6, to better distinguish the individual lines. It clearly shows how the scanlines are following offsets from the geometry boundary. Similar scanlines would be made for finish passes, except the pitch should be smaller.

area containing the alignment mark, and by digital image correlation, it will detect the shift of the image's position, which it subsequently corrects by a beam shift.

2.4. Cross section cut

To be able to determine the topographic features, the straight rectangular sections were filled with FIB induced deposition of platinum, and subsequently cut with multistep cross-sectional patterns and cleaning cross sections at 26 pA.

3. Results

Due to the different beam currents used for different sub patterns in job $A3$, the time for patterning is different. The milling time is equal to the sum of the dwell time for each dwell point for a given pattern. A bar plot in figure 4 illustrates the time used to make the individual patterns. Pattern $A2$ takes only a little longer than $A1$, due tomoverlapping patterns. Pattern $A3$ uses much less time for the bulk milling since it employs a higher beam current, giving it the fastest milling time in total. Additional time is needed for creating alignment marks prior to milling, and for changing and aligning between changing currents.

From figure 3 one can see a major difference in quality of the different patterns. Based on a qualitative analysis, one can see more distinct features in image e) and image f) in figure 3, such as around the corners and pointy intersection

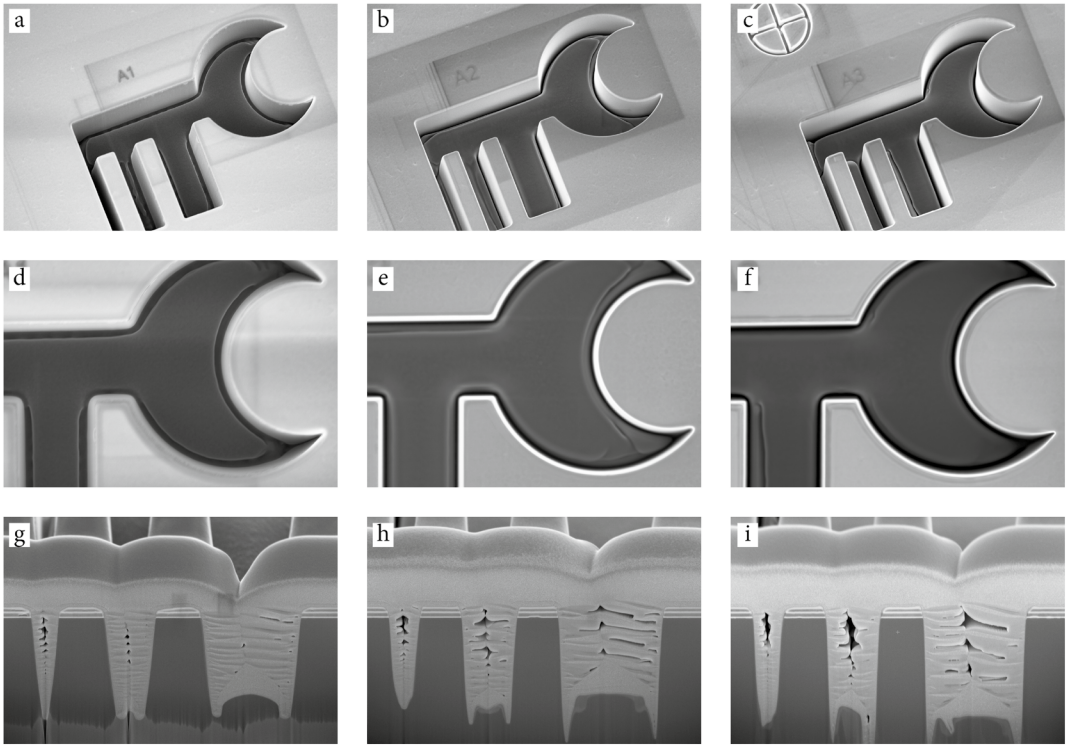

Fig. 3. SEM images. First, second and third column show the same detailed images of sample *A*1, *A*2 and *A*3. Firt row show images taken at 30° tilt angle, second row is a close up image, and third row is a cross sectional image taken at 45° tilt with tilt correction. Image c) also shows the markings used for alignment.

between the two circles along the boundary. Cross-sectional images show a higher sidewall angle along the different grooves in *A*3 and *A*2, compared to *A*1.

These results suggest that splitting the patterning of a geometric object into a bulk milling, and finish passes along that follow the boundary will give more distinct features, and higher angle sidewalls.

4. Discussion

For this study, we designed a simple geometry with a few geometric features that would help demonstrate some aspects of the milling, limiting to sidewall angle and processing time. The chosen beam currents, and finish pass thickness and pattern overlap were selected such that the patterns would show differences with respect to the chosen measures. Further work could be put into optimizing the choice of parameters. That leads to a question of what is optimal. Since milling time and geometric accuracy are inversely related by beam current, there will always be some trade-offs to be made. A multi-objective analysis could reveal a set of optimal solutions, and the right solution can be chosen based on the right trade off.

To demonstrate the principle of this milling strategy, we only changed the beam condition by varying beam current as this has a big impact on both processing time and feature accuracy, and thus nice for demonstration. However, the process can easily be expanded to vary the acceleration voltage (AV) as well. This is a very important aspect in FIB milling, as it has a huge impact on the damage to the sample. In the case of a crystalline material, the damage layer could include an amorphous layer and further defects and impurities in the crystal, whose thickness is nearly proportional to the acceleration voltage. For many samples there will be an upper limit to how thick of a damage layer is acceptable. On the other hand, AV is inversely related to the sputter yield (and thus milling time). Lower AV will

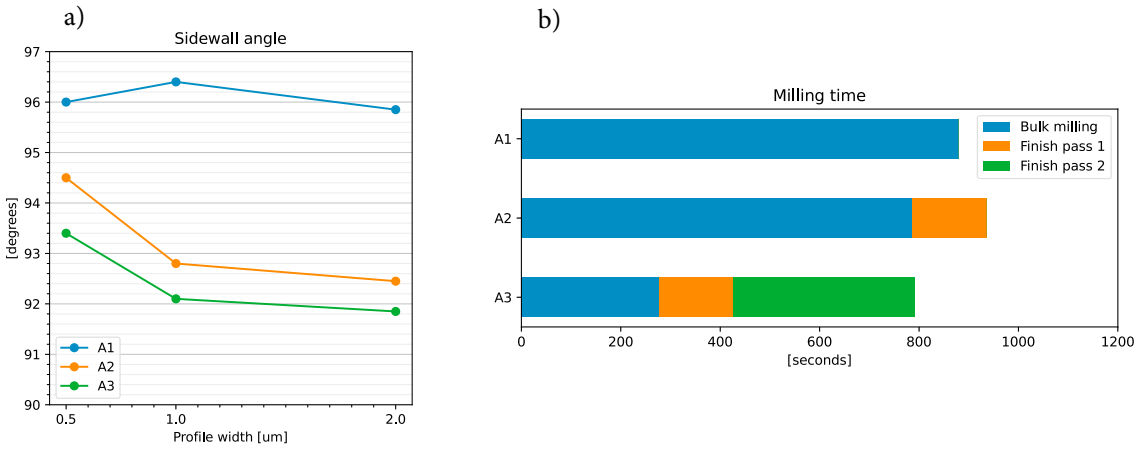

Fig. 4. a) Sidewall angle for different samples at for the different channel widths. Each data point is an average between the two opposing walls. b) Milling time for each of the patterns and sub-patterns.

also increase the beam size.The benefits with the multi-pattern milling strategy is closely linked with the trade-off behavior with changing BC and AV. Further work should be put into optimizing the selection of beam- and patterning parameters for a multi-stage milling strategy.

We also limited ourselves to the aspect of sidewalls. Work should also be put into strategies for improving the dimensional accuracy and quality of bottom surface of a milled structure. Although we have been able to create straight wall segments which should have minimal amounts of redeposition, we expect that the bottom surface will have large amounts.

5. Conclusion

Splitting the patterning job into multiple sub-patterns which scans along offsets of the boundary geometry can be used to get more distinct features and higher angle sidewalls compared to a more conventional milling strategy. By using different beam conditions for different sub-jobs we were able to create a higher quality result in a shorter milling time, compared to all other strategies in our test. This represents a promising strategy for creating complex nano-structures with increased accuracy and quality at a higher throughput rate. In principle, the biggest advantage will come with a high area to boundary length ratio, where the finished sidewall quality must be good.
This paper has simply demonstrated the possibility of improving the sidewall quality by using finish passes at a lower beam current, but the same technique should also work with reducing the acceleration voltage to reduce damage layer induced by the collision cascade in the target material. The method can also be improved to include a combined strategy for improving both the sidewalls and bottom surface of the milled geometry.

Acknowledgements

The Research Council of Norway is acknowledged for the support to the Norwegian Micro- and Nano-Fabrication Facility, NorFab.

Markus Lid acknowledges support from Stanford's NPL-Affiliate Program.

References

Bachmann, M.D., 2020. Focused ion beam micro-machining, in: Manipulating Anisotropic Transport and Superconductivity by Focused Ion Beam Microstructuring. Springer, pp. 5–33.

Chen, X., Ren, Z., Zhu, Y., Wang, Y., Zhang, J., Wang, X., Xu, J., 2020. Formation mechanism and compensation methods of profile error in focused ion beam milling of three-dimensional optical microstructures. SN Applied Sciences 2, 1–16.

Cui, R., Shalaginov, M., Kildishev, A.V., 2017. Nanocraft-fibstream: Focused ion beam stream file generator. URL: https://nanohub.org/resources/fibstream, doi:doi:10.4231/D3DN3ZX26.

Deinhart, V., Kern, L.M., Kirchhof, J.N., Juergensen, S., Sturm, J., Krauss, E., Feichtner, T., Kovalchuk, S., Schneider, M., Engel, D., et al., 2021. The patterning toolbox fib-o-mat: Exploiting the full potential of focused helium ions for nanofabrication. Beilstein journal of nanotechnology 12, 304–318.

Lin, Y., Joy, D.C., 2005. A new examination of secondary electron yield data. Surface and Interface Analysis: An International Journal devoted to the development and application of techniques for the analysis of surfaces, interfaces and thin films 37, 895–900.

Mulders, J., De Winter, D., Duinkerken, W., 2007. Measurements and calculations of fib milling yield of bulk metals. Microelectronic engineering 84, 1540–1543.

Niessen, F., Nancarrow, M.J., 2019. Computer-aided manufacturing and focused ion beam technology enable machining of complex micro-and nano-structures. Nanotechnology 30, 435301.

Utke, I., Moshkalev, S., Russell, P., 2012. Nanofabrication using focused ion and electron beams: principles and applications. Oxford University Press. p. 384.

Yoon, H.S., Kim, C.S., Lee, H.T., Ahn, S.H., 2017. Advanced scanning paths for focused ion beam milling. Vacuum 143, 40–49.